DR YIJI XIA (Orcid ID : 0000-0002-9543-8341)

Article type : Original Article

Redox-sensitive bZIP68 plays a role in balancing stress tolerance with growth in Arabidopsis

Yimin Li[1,2,$], Wuzhen Liu[1,$], Huan Zhong[1,$], Hai-lei Zhang[1], Yiji Xia[1,3,4,5*]

[1]Department of Biology, Hong Kong Baptist University, Hong Kong

[2]College of Pharmacy, Shaanxi Qinling Application and Development and Engineering Center of Chinese Herbal Medicine, Shaanxi University of Chinese Medicine, Xi'an, China

[3]Partner State Key Laboratory of Environmental and Biological Analysis, Hong Kong Baptist University, Hong Kong

[4]State Key Laboratory of Agricultural Biotechnology, Chinese University of Hong Kong, Hong Kong

[5]State Key Laboratory of Environmental and Biological Analysis, Hong Kong Baptist University, Hong Kong

[$]These authors contributed equally to the article.

[*]Corresponding author: Yiji Xia

Tel: 852-34117052

Email: yxia@hkbu.edu.hk

ORCID ID: 0000-0002-9543-8341 (Y.X.).

This article has been accepted for publication and undergone full peer review but has not been through the copyediting, typesetting, pagination and proofreading process, which may lead to differences between this version and the Version of Record. Please cite this article as doi: 10.1111/tpj.14476

Running head: bZIP68 balances stress tolerance with growth

Key words: bZIP68, transcriptional regulation, oxidative stress, seedling growth, *Arabidopsis thaliana*

ABSTRACT

Perturbation of the cellular redox state by stress conditions is sensed by redox-sensitive proteins so that the cell can physiologically respond to stressors; however, the mechanisms linking sensing to response remain poorly understood in plants. Here we report that the transcription factor bZIP68 underwent in vivo oxidation in Arabidopsis cells under oxidative stress which is dependent on its redox-sensitive Cys320 residue. bZIP68 is primarily localized to the nucleus under normal growth conditions in Arabidopsis seedlings. Oxidative stress reduces its accumulation in the nucleus and increases its cytosolic localization. Chromatin immunoprecipitation followed by sequencing (ChIP-seq) revealed that bZIP68 primarily binds to promoter regions containing the core G-box (CACGTG) or G-box-like motif of the genes involved in abiotic and biotic stress responses, photosynthesis, biosynthetic processes, and transcriptional regulation. The *bzip68* mutant displayed slower growth under normal conditions but enhanced tolerance to oxidative stress. The results from the ChIP-seq and phenotypic and transcriptome comparison between the *bzip68* mutant and wildtype indicate that bZIP68 normally suppresses expression of stress tolerance genes and promotes expression of growth-related genes, whereas its inactivation enhances stress tolerance but suppresses growth. bZIP68 might balance stress tolerance with growth through the extent of its oxidative inactivation according to the environment.

INTRODUCTION

The cellular redox state is determined by the delicate balance between production and scavenging of reactive oxygen species (ROS) (Foyer and Noctor, 2005; Moller et al., 2007; Finkel, 2011; Collins et al., 2012). The anti-oxidant defense system, which includes small antioxidants and antioxidant enzymes, is effective in maintaining cellular redox homeostasis under normal growth conditions. However, biotic and abiotic stresses can cause overproduction of ROS, thereby disturbing redox homeostasis and causing oxidative damage to biomolecules. Living organisms have evolved mechanisms to use ROS as signal molecules to mediate stress responses and developmental processes (Apel and Hirt, 2004; Foyer and Noctor, 2005; D'Autreaux and Toledano, 2007; Moller et al., 2007; Finkel, 2011; Schieber and Chandel, 2014).

ROS act as signals largely by oxidatively modifying redox-sensitive proteins that function as molecular switches (Georgiou, 2002; D'Autreaux and Toledano, 2007; Finkel, 2011; Schieber and Chandel, 2014). Thiols in some cysteine residues are particularly sensitive to oxidation. A change in the redox status of such a protein might alter its activity, stability, or subcellular localization. Several transcription factors in microorganisms have been characterized as redox sensors that regulate oxidative stress tolerant genes. For instance, yeast AP-1-like transcription factor (YAP1), a member of the basic leucine zipper protein family (bZIP), translocates when oxidized from the cytosol to the nucleus, where it activates genes encoding oxidative stress tolerance proteins (Kuge et al., 1997). Some signaling components and transcriptional regulators involved in plant stress responses have also been found to be regulated through their oxidation/reduction [reviewed by (Dietz, 2014;

Herrera-Vasquez et al., 2015)], including NON-EXPRESSOR of PR1 (NPR1) and a few TGA transcription factors in Arabidopsis (Mou et al., 2003; Lindermayr et al., 2010).

Stress conditions often cause energy deficiency. It is vital for plants to re-establish cellular homeostasis to balance growth and stress responses in accordance with the environmental conditions. ROS is believed to play key signaling roles in the interplay between hormone-mediated stress responses and growth regulation in plants (Foyer and Noctor, 2005; Moller et al., 2007; Marino et al., 2012; Xia et al., 2015). The specificity of ROS signaling might be achieved through a combination of distinct ROS production signatures under different stress conditions, such as amplitude, duration, and cellular compartments. It remains largely unknown how plants perceive stress through redox perturbation and then connect the sensory networks to the transcriptional regulatory networks to balance growth and stress tolerance.

Previously, we developed a redox proteomics approach termed oxiTRAQ for identifying redox-sensitive proteins in Arabidopsis (Liu et al., 2014). bZIP68 and G-box Binding Factor 1 (GBF1) were among the identified redox-sensitive proteins that underwent reversible oxidative modifications in Arabidopsis suspension cells after hydrogen peroxide treatment. bZIP68, GBF1, and bZIP16 belong to the G subgroup of the bZIP superfamily of proteins in Arabidopsis (Jakoby et al., 2002), and their DNA binding activities were found inhibited by *in vitro* ROS treatment but enhanced by DTT treatment, likely through redox-regulation of their conserved cysteine residues (Shaikhali et al., 2012). GBF1 and bZIP16 were reported to regulate genes involved in responses to light, phytohormones, and stresses (Schindler et al., 1992; Garreton et al., 2002; Shen et al., 2008; Smykowski et al., 2010; Hsieh et al., 2012;

Shaikhali et al., 2012). The loss-of-function mutation of bZIP68 was found to cause reduction in the transcript level of *LHCB2.4* (Shaikhali et al., 2012); however, the bZIP68's biological function and other genes regulated by bZIP68 remain unknown. This report presents our findings which suggest that bZIP68 might play a role in sensing oxidative stress to mediate transcriptional reprogramming to balance plant growth and stress tolerance.

RESULTS

bZIP68 undergoes in vivo oxidation under H_2O_2 treatment which is dependent on its Cys320 residue

bZIP68 contains two cysteine residues, Cys182 and Cys320. To further reveal whether bZIP68 undergoes oxidative modification under oxidative stress in vivo and which cysteine residue is sensitive to oxidative stress, we mutated C182 or C320 to serine, fused the wildtype and the mutated genes with the HA tag, and transiently expressed the fusing constructs in protoplasts from Arabidopsis leaves under the control of the 35S promoter. The protoplasts transformed with bZIP68-HA were treated with 5 mM H_2O_2, DTT, or the buffer only (as a mock control) for 60 minutes. Proteins were extracted from the protoplast. The loading buffer with or without DTT was added to the protein samples which were then separated by SDS-PAGE and detected by the anti-HA antibodies through Western blot analysis. Without the reducing agent DTT in the loading buffer, intra- or inter-protein disulfide bonds were expected to be retained. In the mock-treated protoplasts transformed with bZIP68-HA, in addition to the band similar in size to the expected bZIP68-HA (44 kDa),

two other bands of approximately 60 kDa and 150 kDa were also detected (Fig 1a). However, in the DTT-treated protoplasts, the 150 kDa band was undetectable. In contrast, in the H_2O_2-treated protoplasts, the 150 kDa band was the dominant form but the 44 kDa and 60 kDa bands were not detected. The result indicates that the 150 kDa band contained an oxidized form of bZIP68-HA which could be a homo- or hetero-multimer. The 44 kDa and 60 kDa bands were likely the reduced forms and the latter could be a post-translationally modified form of bZIP68-HA. The treatment of the protoplasts with methyl viologen (MV, an inducer of oxidative stress) did not lead to striking difference in the band pattern except the 60 kDa band became much weaker (Fig 1a), perhaps because MV, which is known to induce ROS production in chloroplasts under illumination, did not induce a much higher level of ROS in the protoplasts which were placed under dim light. If the protein extracts were added with the loading buffer containing DTT, the 150 kDa band was not detected in the protoplasts under all those treatments (Fig 1a). The results indicate that bZIP68 underwent a reversible oxidative modification in vivo under the oxidative stress.

In the protoplasts transformed with bZIP68C320S-HA, the 150 kDa band was not detected either under the mock or H_2O_2 treatment although a faint band of approximately 220 kDa with unknown nature appears in the H_2O_2-treated protoplasts (Fig 1b). The result indicates that oxidation of bZIP68 is dependent on the Cys320 residue. The protein band patterns detected in the protoplasts expressing bZIP68-C182S were similar to those in the bZIP68-HA-transformed protoplasts; however, the level of bZIP68C182S-HA was much lower than bZIP68-HA, suggesting that the C182S mutation did not affect oxidation of

bZIP68-HA but made the protein less stable. The C182S and C320S double mutation further reduced the protein level.

To examine whether bZIP68 could also undergo oxidative modification in seedlings under other abiotic stresses. Transgenic seedlings expressing 35S promoter:bZIP68-FLAG fusion were grown under the half-strength (1/2) Murashige and Skoog (MS) medium for seven days and then transferred to new MS medium containing H_2O_2, MV, NaCl, or ABA or transferred to a high temperature (37 °C) condition. One hour after the stress treatment, the seedlings were harvested and extracted proteins were subjected to Western blotting analysis. In addition to H_2O_2, the treatments with MV, NaCl, and ABA also caused some bZIP68-FLAG to be oxidized but to a lesser degree compared to oxidation caused by H_2O_2 (Supplementary Figure S1).

Oxidative stress affects subcellular localization patterns of bZIP68-eYFP

bZIP68 is predicted by the PSORT algorithm (http://psort1.hgc.jp/form.html) to contain a nuclear localization signal (NLS). For experimental verification of subcellular localization of bZIP68, we generated transgenic Arabidopsis lines that expressed bZIP68 fused with enhanced yellow fluorescent protein (eYFP) to its C-terminus under the control of either the *bZIP68* promoter (*bZIP68pro:bZIP68-eYFP*) or the 35S promoter (*35S:bZIP68-eYFP*). The YFP signal was primarily localized in nuclei under the normal growth condition in root and leaf cells of these transgenic lines (Fig 2a, 2b, and Fig S2a, S2b, S2c, and S2e). Similar

subcellular localization patterns were observed in the *bZIP68pro:bZIP68-eYFP* lines and the *35S:bZIP68-eYFP* lines although the YFP signal was generally stronger in the latter.

The seedlings of these bZIP68-eYFP reporter lines were exposed to oxidative stress by treating them with 5 mM H_2O_2. In the *bZIP68pro:bZIP68-eYFP* lines, within approximately 30 minutes after the ROS treatment, the YFP fluorescence signal became reduced in nuclei but appeared in the cytoplasm of some cells in the roots (Fig 2c, 2d). Longer H_2O_2 treatment often led to redistribution of the YFP signal in more cells. In the *35S:bZIP68-eYFP* lines, the YFP signal often largely remained in the nucleus while also appearing in the cytoplasm in some root cells following ROS treatment (Fig S2b), perhaps due to the higher level of bZIP68-eYFP expression in those lines. In pavement cells of leaves in the *35S:bZIP68-eYFP* lines, following the ROS treatment, the YFP signal was re-localized primarily to the cytoplasm; however, in guard cells, the signal was generally detected in both the nucleus and the cytoplasm (Fig S2d, S2f). Besides, it appeared that the redistribution was more readily detected in epidermal cells than in the inner layer cells, perhaps due to more exposure of the epidermal cells to H_2O_2 under the treatment. It was difficult to precisely quantify the number of cells that showed redistribution of the YFP signal at a given time as the process was dynamic. We estimated that approximately 30% of epidermal cells in the cell division and elongation zones of roots showed redistribution of the YFP signal in 30 minutes after the ROS treatment. However, it remains to be determined whether the redistribution of the bZIP68-eYFP under the ROS treatment was due to its nucleocytoplasmic shuttling or due to its degradation in the nucleus and re-synthesis in the cytosol.

To examine whether the redistribution of bZIP68 under oxidative stress is dependent on Cys320, we generated transgenic lines expressing *35S:bZIP68C320S-eYFP*. Like the wildtype bZIP68, bZIP68C320S-eYFP was localized in nuclei under the normal condition (Fig 1e, 1f). However, under the oxidative stress treatment, bZIP68C320S-eYFP remained primarily in the nuclei (Fig 1g, 1h).

The *bzip68* mutation causes slower seedling growth

Other than the previous report that a loss-of-function mutation of bZIP68 caused reduced expression of *LHCB2.4* (Shaikhali et al., 2012), biological function of *bzip68* has not been reported. We obtained two T-DNA insertion lines for the *bZIP68* gene. *bzip68-1* carries a T-DNA insertion in the first exon (8 bases downstream of the transcription start site), whereas *bzip68-2* has an insertion in exon 11 (Fig S3a). Through reverse transcription real-time PCR (qPCR) analysis using the primer pair qF1 and qR1 (Fig S3a), it was found that the *bZIP68* transcript in the *bzip68-1* mutant was barely detectable (Fig S3b), indicating that *bzip68-1* is a knockout or a severe knockdown allele, a notion that was later confirmed by the RNA-sequencing (RNA-seq) data (see below). As expected, the transcript was not detected from the *bzip68-2* mutant in the qPCR analysis (Fig S3b) as the primer qR1 is located downstream of the insertion site (Fig S3a). However, the region upstream of the T-DNA insertion was still transcribed from *bzip68-2* (Fig S3c).

When grown in soil, the *bzip68-1* mutant plants were smaller than wildtype plants and showed a slight delay in flowering (Fig 3a, 3b). Although the *bzip68-2* mutant was also smaller than wildtype, the difference was less significant. In subsequent phenotypic analysis, the differences between the *bzip68-2* mutant and the wildtype plants were often found not significant or less significant compared to the difference between *bzip68-1* and wildtype, suggesting that *bzip68-2* is a weaker allele. In rest of this report, the *bzip68*-2 mutant is not included, and *bzip68-1* is abbreviated as *bzip68*.

When grown on the MS medium containing 1% (MS 1) or 3% (MS 3) sucrose, the mutant also grew slower than wildtype (Fig 3d-3f). The differences in growth rates were more obvious during the young seedling stages (in about the first 10 days) but remained throughout the later stages.

Wildtype and *bzip68* were subjected to various abiotic and biotic stress treatments, including salt stress (100 mM NaCl), osmotic stress (100 mM sorbitol), and flg22 (a peptide from bacterial flagellin that induces the defense response). The seedling growth phenotype was not strikingly more different between the mutant and wildtype seedlings under these treatments compared to the differences without these stress treatments. When seedlings were grown on the medium under lower light intensity (approximately 30 mol m^{-2} sec^{-1}) vs. the normal light condition (125 mol m^{-2} sec^{-1}), the mutant showed a slower growth rate compared to wildtype (Fig 3g-3i). Similarly, when seedlings were grown under low temperature (14-16 °C), growth of the *bzip68* mutant was more severely inhibited than that of wildtype (Fig 3j-3l). In addition, more pronounced purple pigmentation was seen in the *bzip68* seedlings than in the wildtype seedlings under low temperature (Fig 3k). The slower

growth phenotype of the *bzip68* mutant under the various conditions in soil and on the media could be genetically complemented by the genomic clone of *bZIP68* (Fig S4a-S4d).

The *bzip68* mutation enhances tolerance to oxidative stress

To determine whether the *bzip68* mutation alters tolerance to oxidative stress, we initially germinated seeds and grew seedlings on the medium containing H_2O_2. The difference in seedling growth phenotypes between the mutant and wildtype was similar to that under the normal growth medium. As H_2O_2 is unstable and might not be suitable for phenotypic analysis under long-term oxidative stress treatment, we tested seedling growth phenotypes in presence of MV on the growth medium. MV, an herbicide also known as paraquat, catalyzes the transfer of electrons from photosystem I to oxygen leading to ROS production (Chia et al., 1982; Babbs et al., 1989) and is commonly used to induce oxidative stress. As shown in Fig 4, although the *bzip68* seedlings grew slower than wildtype seedlings on the MS3 medium, they grew better than wildtype in the presence of low concentration of MV (10-25 nM) (Fig 4a, 4b). Higher concentration of MV severely inhibited growth of both *bzip68* and wildtype seedlings and their difference became statistically insignificant. The *35S:bZIP68-FLAG* transgenic line (in the Col-0 background) displayed more severe growth inhibition by MV than wildtype (Fig 4a, 4b).

Identification of genome-wide bZIP68 binding regions by chromatin immunoprecipitation followed by high-throughput sequencing (ChIP-seq)

To identify bZIP68's direct target genes, ChIP-seq analysis was performed using the transgenic Arabidopsis plants expressing the 35S:bZIP68-FLAG fusion protein in the *bzip68* background. The anti-FLAG antibodies were used in the ChIP experiment which included three biological replicates and a Col-0 wildtype line expressing 35S:GFP-FLAG as a negative control. A total of 5,748 bZIP68-bound regions (peaks) (Table S1) were identified and these peaks are associated with 1,058 Arabidopsis genes. As expected for most transcription factors, over 80% the peaks are associated with the typical gene promoter regions [-1.0 kb to +500b relative to transcription start sites (TSS)] and are highly concentrated around -100 bp of TSS (Fig 5a, 5b). We further focused on 896 strongest binding peaks (p value ≤ 1e-30) that are located within 1.5 kb upstream and 500 bp downstream of TSS for further analysis. These peaks are associated with 892 genes (Table S2). Using the HOMER motif analysis algorithm to search motifs on these peaks, the G-box and G-box-like motifs were found to be the most enriched motifs (Fig 5c). These motifs have previously been known to be bound by the G-group of Arabidopsis bZIP superfamily as well as by some basic helix–loop–helix transcription factors (bHLH) including PHYTOCHROME-INTERACTING FACTOR 4 (PIF4) and PIF5, SPEACHLESS (SPCH), INCREASED LEAF INCLINATION 1-BINDING bHLH1 (IBL1), and BZR1/BES1 that are known to regulate growth, development, and responses to light, stresses, and phytohormones (Yu et al., 2011; Oh et al., 2012; Shaikhali et al., 2012; Lau et al., 2014; Pfeiffer et al., 2014; Zhiponova et al., 2014).

Gene ontology (GO)-based analysis of these genes revealed that the significantly enriched GO terms include the genes involved in transcriptional regulation, responses to abiotic and biotic stimuli and ABA, photosynthesis, oxidation-reduction process, and protein/RNA metabolic processes (Fig 5d and Table S3). Several genes encoding antioxidant proteins, such as peroxidase, superoxide dismutase, and glutathione peroxidase, were associated with the bZIP68 binding peaks.

To verify the ChIP-seq data, we selected promoter regions of twelve genes that were found to be associated with the bZIP68-binding peaks for ChIP-qPCR analysis. ChIP was conducted using transgenic plants expressing either 35S:bZIP68-FLAG or 35S:GFP-FLAG (as a control). The promoter of bZIP68 was found to be bZIP68-bound in the ChIP-seq analysis, suggesting that it is self-regulated. The ChIP-qPCR analysis showed slightly enrichment of its promoter region in the bZIP68-FLAG-precipitated sample but the difference was not statistically significant (Fig 6a). The promoter regions in the other 11 genes were found to be significantly enriched through immunoprecipitation by bZIP68-FLAG (Fig 6a). One of them is *bZIP60*. *bZIP60* transcripts are known to undergo alternative splicing and intercellular movement to facilitate systemic ER stress (Deng et al., 2011; Lai et al., 2018). Another gene is *ERF109* (*ETHYLENE RESPONSE FACTOR 109*) which is also known as *RRTF1* (*REDOX RESPONSIVE TRANSCRIPTION FACTOR 1*) (Cai et al., 2014; Matsuo and Oelmüller, 2015). Five of them (*GOLS1, GOLS2, GOLS3, RFS5, RFS6*) encode proteins involved in the galactinol and raffinose biosynthetic pathway. Galactinol and raffinose have been reported to protect plants from oxidative stress caused by paraquat (Nishizawa et al., 2008).

We also selected promoter regions of another two genes in the ChIP-qPCR assay. These two genes, *NDL2* (*N-MYC DOWNREGULATED-LIKE 2*) and *DREB1F* (*DEHYDRATION ELEMENT-BINDING FACTOR 1F*), were found differentially expressed between the *bzip68* mutant and wildtype based on RNA-seq analysis (see below) but were not found to be associated with the bZIP68-binding peaks. From the ChIP-PCR assay, their promoter regions were also not enriched in the bZIP68-FLAG-precipitated DNA fragments (Fig 6a), indicating that they might be indirectly regulated by bZIP68.

To further verify the ChIP-seq and ChIP-qPCR data, a 54-bp DNA fragment from each promoter region of six genes (Fig S5) associated with the bZIP68-bound peaks were synthesized and used as probes for electrophoresis mobility shift assay (EMSA). For the assay, bZIP68 fused with the His tag was expressed in and purified from *E. coli* (Fig S6). As shown in Fig 6b, His-bZIP68 bound to all of these six DNA fragments. Strong binding was detected for the DNA probes from *GOLS2*, *GOLS3*, *At5g05220*, and *OBAP2A* whereas bZIP68's binding to the DNA probes from *ERF109* and *At5g15500* was relatively weaker.

The *bzip68* mutation enhanced expression of stress-responsive genes

High-throughput RNA-sequencing (RNA-seq) was employed to generate transcriptome profiles of the *bzip68* mutant and wildtype seedlings. We compared the differences in transcriptome profiles of 2-week-old mutant and wildtype seedlings grown on MS3 medium 90 minutes after treatment with 5 mM H_2O_2 or H_2O (mock). Transcriptome profiles were also generated for 2-week-old mutant and wildtype seedlings grown on MS3 medium under low

light intensity (30 mol m^{-2} sec^{-1}). Genes whose expression levels showed at least 1.5 fold difference [with a false discovery rate (FDR)-adjusted *p*-value ≤ 0.05] in a comparison between two samples were considered differentially expressed genes (DEGs) in this report. Supplementary Table 1 (Table S4) lists all DEGs according to at least one of the comparisons between the wildtype and *bzip68* seedlings under the same condition or between mock and ROS treatment in the same genotype. The RNA-seq data have been deposited to the NCBI GEO database (BioProject PRJNS412712).

Under the low light condition, 523 genes were up-regulated and 161 down-regulated in the *bzip68* seedlings compared to wildtype. Among the DEGs with a higher expression level in the mutant, GO enrichment analysis revealed that the most significantly enriched GO terms (Table 1, Table S5) were stress-responsive genes, including responses to both biotic and abiotic stresses. Among the down-regulated genes by the mutation, the most significantly enriched GO terms included auxin-response and auxin transport, stress responses, and karrikin response. Karrikins were initially identified in burnt plant materials and are perceived by cellular receptors to promote seed germination and seedling growth (Waters et al., 2014; Flematti et al., 2015; Meng et al., 2016; Morffy et al., 2016). The transcript level of *LHCB2.4* was also significantly decreased in the *bzip68* mutant, consistent with the previous report that bZIP68 acts as its transcriptional activator of *LHCB2.4* (Shaikhali et al., 2012). A number of genes involved in oxidative stress responses are among the DGEs, including a dozen of peroxidase genes and GST genes and a few glutathione peroxidase genes.

Table S6 lists 80 genes that were most highly upregulated and another 80 genes most highly down-regulated in the mutant relative to the wildtype under the low light condition. Among the genes most up-regulated by the *bzip68* mutation include several genes encoding antioxidant proteins, many genes involved in abiotic and biotic stress responses, several ethylene-responsive transcription factor (*ERF*) genes, and several genes in light response. Among the most down-regulated genes in the *bzip68* mutant include those involved in auxin transport [such as *NDL2* and *PINOID-BINDING PROTEIN 1* (Benjamins et al., 2003; Mudgil et al., 2009)], several *ERF*s, several genes related to cell expansion, a few genes involved in light responses, and a gene encoding trehalose-phosphate phosphatase (TPPD).

Mock (H_2O) treatment was used as a control for the H_2O_2 treatment to analyze H_2O_2-responsive genes in seedlings grown under normal light intensity. Comparing the mock-treated *bzip68* and wildtype samples, a total of 250 genes were found to have significantly different levels of expression between the mutant and wildtype. Among these DEGs, 70 genes were expressed at a higher level, and 170 genes were at a lower level in the mutant compared to wildtype. This number is lower than the number of the genes showing differential expression between the two genotypes under the low light condition, which is consistent with the more pronounced phenotypic difference between the mutant and wildtype under low light condition compared to normal light. It could also be due to the difference in the developmental stages of seedlings, as the seedlings under the low light condition developed slower than those under the normal light and the *bzip68* mutation affects growth at earlier seeding stages more than at later stages.

The transcriptome profile of the *bzip68* mutant resembles that of oxidatively stressed plants

In response to the H_2O_2 treatment in the wildtype seedlings, 527 genes and 189 genes were found to be up- and down-regulated, respectively. These DEGs (H_2O_2-responsive genes) (listed in Table S7）were termed H_2O_2-induced and H_2O_2-suppressed genes, respectively. The results of GO enrichment analysis of the H_2O_2-responsive genes in wildtype are shown in Table 2 and Table S8. The most common GO enrichment terms among the H_2O_2-induced genes are those known to respond to heat shock, hydrogen peroxide, and other abiotic and biotic stresses, whereas the most common types of H_2O_2-suppressed genes include those involved in the response to light, circadian rhythm, karrikins, gibberellins, and various stresses, and in cell division.

Among the 523 genes mentioned earlier that were expressed at a higher level in the *bzip68* mutant compared to wildtype under low light, 262 were H_2O_2-induced genes and 19 were H_2O_2-suppressed genes. Among the 161 genes with a lower expression level in the mutant compared to the wildtype, 67 were H_2O_2-suppressed and 28 H_2O_2-induced. The above results indicate that the up-regulated genes in the *bzip68* mutant tend to be H_2O_2-inducible, whereas the *bzip68* down-regulated genes to be H_2O_2-suppressed. Such a notion is also supported from the hierarchical clustering (heatmap plot) of DEGs between those samples (Fig 7a), which shows that the wildtype plants under H_2O_2 treatment had a similar gene expression pattern to that of the *bzip68* mutant (under low light without H_2O_2 treatment).

Comparing the H_2O_2-treated wiltype and H_2O_2-treated *bzip68* seedlings, the H_2O_2-induced genes in wildtype were generally also induced by H_2O_2 in the *bzip68* mutant; similarly, the H_2O_2-suppressed genes were also generally suppressed in the mutant by H_2O_2 (Table S4 and Fig 7a). The total number (922) of H_2O_2-responsible genes in the mutant was higher than the number (716) in wildtype. The H_2O_2-induced genes tend to be induced to a higher level by H_2O_2 in *bzip68* than in wildtype. For the H_2O_2-suppressed genes, the difference was less obvious. Overall, the result further indicated that the *bzip68* mutation enhances the expression patterns of H_2O_2-responsive genes.

The number of the genes associated with bZIP68-bound peaks identified from the ChIP-seq analysis was larger than the number of the DEGs between the *bzip68* mutant and wildtype identified from the RNA-seq analysis (Table S1, S2, S4, and Fig S7). Fifty-three of the 892 genes associated with bZIP68 bind sites were among the DGEs (Fig S7). The result suggests that expression of most of the DGEs between *bzip68* and wildtype were indirectly affected by the *bzip68* mutation. Alternatively, bZIP68 might be expressed in a low number of cells and the profiling analysis of the transcriptomes from the whole seedlings was not sufficiently sensitive for identifying many bZIP68-regulated genes. It is also possible that not all bindings of bZIP68 lead to detectable changes in gene expression.

For confirmation of some of the RNA-seq data, we selected six DEGs for analysis by reverse transcription qPCR (RT-qPCR) to further compare their transcript levels between *bzip68* and wildtype. These six genes included *NDL2, ENT1, NOP5-2, CDC68-related, At5g13120, and NAC044*. The transcript levels of five of these genes detected by RNA-seq and qPCR were found overall consistent (Fig 7b). However, the result on the transcript level

of *NAC044* from the RT-qPCR analysis was not consistent from that of the RNA-seq data. *bZIP68* was also selected in the analysis and as expected, its transcript level in the mutant was much lower than in wildtype.

Two other genes, *At5g05520* and *ERF109* were found to be associated with the bZIP68-binding peaks based on the ChIP-seq, ChIP-PCR, and EMSA results; however, no significant difference in their transcript levels was detected between the mutant and wildtype in the RNA-seq analysis (Fig 7b). They were also selected in the RT-qPCR analysis but were not found to be differentially expressed under the experimental conditions. The result was not surprising as it is expected that not all bZIP68-regulated genes would show differential expression under certain conditions.

Among the H_2O_2-responsive genes identified from the RNA-seq analysis, we selected four genes for verification by RT-qPCR. Three of them (*DREB1F*, *ERF109*, *At5g05220*) were also associated with the bZIP68-binding peaks. As shown in Fig 7c, these four genes were significantly induced in both wildtype and *bzip68-1* seedlings upon H_2O_2 treatment. Two of them, *At1g71000* and *At5g05220*, also showed higher levels of expression in the *bzip68* seedlings than in wildtype under the H_2O_2 treatment.

DISCUSSION

Adverse environmental conditions are known to result in excessive production of ROS, leading to oxidative stress. Living organisms have evolved complex mechanisms to sense oxidative stress and activate appropriate physiological and developmental responses. Redox signaling is apparently initiated by redox-sensitive proteins, whose function can be switched on and off through reduction/oxidation.

The G group members of the bZIP superfamily in Arabidopsis, such as GBF1, bZIP16, and bZIP68, have been found to bind to the G-box and their in-vitro DNA binding ability is sensitive to ROS (Shaikhali et al., 2012) (Schindler et al., 1992; Shen et al., 2008; Hsieh et al., 2012), indicating that they might function in sensing cellular redox states. bZIP68 was previously found in our redox proteomics analysis to undergo oxidative modifications in Arabidopsis suspension cells under H_2O_2 treatment (Liu et al., 2014). Here, we showed that bZIP68 also underwent reversible oxidation in protoplasts under H_2O_2 treatment which is dependent on its redox-sensitive Cys320 residue. Cys320 could be directly oxidized by H_2O_2 or by a redox-sensitive protein (such as a peroxiredoxin). Treatment of seedlings with some abiotic stresses and ABA could also cause bZIP68 oxidation.

bZIP68 is primarily localized in nuclei under normal growth conditions. In some cells of the H_2O_2-treated seedlings, the bZIP68-eYFP signal disappeared in nuclei and appeared in the cytosol, suggesting that bZIP68 might undergo nucleocytoplasmic shuttling. Alternatively, oxidation of bZIP68-eYFP might alter its fluorescent property rendering it undetectable by confocal microscopy, whereas the fluorescence signal in the cytosol after the ROS treatment

could be from newly synthesized bZIP68-eYFP. There is also a possibility that the change of bZIP68 subcellular localization might not be differently due to its oxidation but involves another signaling event such as phosphorylation.

For bZIP68 to directly sense ROS, ROS would need to be produced in the nucleus or diffused from the cytosol to the nucleus. Mechanisms of nuclear ROS production is unknown although it has been reported in animal cells (Provost et al., 2010). As for translocation of ROS from the cytoplasm to the nucleus, non-radical H_2O_2 could act as such a short-distance signaling molecule as it is less reactive and more stable than radical ROS (Lamb and Dixon, 1997). Recently, it was reported that during stress, stromules of chloroplast can extend and connect to the nucleus which might promote transport of ROS and other molecules (Brunkard et al., 2015; Caplan et al., 2015).

From the ChIP-seq analysis, bZIP68 was found to primarily bind to the G-box and G-box-like cis-elements in promoter regions of the genes involved in transcriptional regulation, abiotic and biotic stress responses, photosynthesis, and biosynthetic processes. Many transcription factors involved in stress responses, particularly in ABA and ethylene responses are among the putative target genes of bZIP68. Transcriptome profiling analysis indicated that the loss-of-function mutation of bZIP68 causes elevated expression of H_2O_2-induced genes and reduced expression of H_2O_2-suppressed genes. Among the most elevated genes in the mutant are those involved in abiotic stress responses, antioxidant systems, and defense. The genes repressed in the mutant include those involved in growth. These results indicate that under normal growth conditions bZIP68 directly or indirectly suppresses stress tolerance genes but enhances growth-promoting genes. Upon sensing

oxidative stress, oxidation of bZIP68 might cause its inactivation and/or its shuttling from the nucleus to the cytosol. This would relieve the bZIP68-mediated repression of stress-tolerance genes but decrease expression of growth-promoting genes. The degree to which bZIP68 proteins become oxidatively inactivated is likely dependent on severity of the oxidative stress encountered by the individual cells and sensitivity of different cells to oxidative stress, thereby fine-tuning the stress response to balance stress tolerance with growth according to environmental conditions.

The *bzip68* seedlings and adult plants grew slower than wildtype. However, under oxidative stress caused by MV, the *bzip68* seedlings grew better than wildtype. The slower growth of the mutant was likely due to elevated expression of stress tolerance genes and reduced expression of growth-promoting genes. bZIP68 likely function to prevent unnecessary expression of stress tolerance genes to enhance growth when the environment is favorable for growth. Under stress, activation of bZIP68 can lead to enhanced expression of stress-tolerant genes at a cost of growth suppression.

Members of homologous transcription factors could have highly overlapping sets of binding sites. Transcription factors of different families can also bind to the same cis-elements. These transcription factors might compete for or co-operatively bind to common cis-elements to fine-tune regulatory networks. Many members of the bZIP family and the basic helix-loop-helix (bHLH) in Arabidopsis, such as HY5, PIF3, PIF4, and PIF5, bind to the highly conserved G-box motif which is present in a large number of genes involved in growth, light responses, stress responses, and phytohormone responses (Menkens et al., 1995; Siberil et al., 2001; Oh et al., 2012; Chen et al., 2013; Toledo-Ortiz et al., 2014;

Ezer et al., 2017). Several G-box-binding proteins (HY5, PIF3, PIF1) coordinate to regulate ROS-response genes in adapting to the light environments (Chen et al., 2013).

In nature, plants are often subjected to a combination of different stresses. Plants need to have complex sensing and signaling networks to fine-tune physiology in response to the ever-changing environment. bZIP16, bZIP68, and GBF1 are known to interact with each other *in vitro* and in the yeast two hybrid system (Shen et al., 2008; Shaikhali et al., 2012). Interestingly, bZIP16 was found to be a transcriptional repressor of LHCB2.4 whereas bZIP68 and GBF1appear to act as its activators (Shaikhali et al., 2012). These redox-sensitive members of the G-group of the bZIP protein family as well as other redox-sensitive transcription factors might form transcriptional regulatory circuits that coordinate interpretation of different oxidative stress signals and transduce them into appropriate physiological responses through transcriptional reprogramming.

EXPERIMENTAL PROCEDURES

Plant Materials and Growth Conditions

Arabidopsis thaliana T-DNA insertion lines *bzip68-1* (SALK_065543) and *bzip68-2* (SALK_094254C) are both in the Col-0 background and were obtained from the Arabidopsis Biological Resource Center (ABRC) (http://abrc.osu.edu/). Homozygous insertion lines were confirmed by genomic PCR analysis using the T-DNA left border primer LBb1 and gene-specific primers (all primers used in this study are listed in supplementary Table 9).

Soil-grown plants were normally placed in a climate-controlled walk-in growth room with the conditions set at 23 ºC ± 2 ºC, 50% humidity, and 125 mol m^{-2} sec^{-1} light intensity provided by cool-white fluorescent bulbs under a 16-h photoperiod. For growing seedlings on agar media, surface-sterilized seeds were plated on medium containing half-strength Murashige and Skoog (MS) Basal Salts (Sigma, M5524-1L), 0.7% agar for horizontal growth or 0.9% agar for vertical growth, 0.05% MES, pH 5.7 (adjusted by 1 M KOH), with other components as specified in the result section. Seedlings in petri dishes were placed in a growth chamber (SANYO, MLR-351H or CONVIRON, E7/2) at 23 ºC (normal temperature) or 15 ºC (low temperature) with 50% humidity and a light intensity of 125 mol m^{-2} sec^{-1} (normal light intensity) or 30 mol m^{-2} sec^{-1} (a low light intensity) under a 16-h light/8-h dark photoperiod.

Constructs for subcellular localization study of bZIP68-eYFP and the bZIP68 point mutations

To generate the *bZIP68-eYFP* fusion under the control of the 35S promoter, a genomic region of bZIP68 was amplified with the primers SalI-35SAtbZIP68-F and 35SAtbZIP68-BamHI-R from Col-0 and cloned into the TA cloning vector pMD-T19 (TaKaRa) to yield pMD-T19/bZIP68. The genomic fragment was then subcloned into the SalI/BamHI-digested pCAM35S:eYFP vector (Lu et al., 2011) to yield *35S::bZIP68-eYFP*. To place *bZIP68-eYFP* under the control of the *bZIP68* promoter, a 3.4-kb (-1164 to +2270) genomic fragment of *bZIP68* was amplified with the primers BamHI-pAtbZIP68-F and pAtbZIP68-AgeI-R and

sub-cloned into a BamHI/AgeI-digested pBAR-eYFP vector to yield *bZIP68pro:bZIP68-eYFP*.

The bZIP68C320S and bZIP68C182S point mutations were generated through site-directed mutagenesis using the overlap extension PCR method (Ho et al., 1989). The pMD-T19/bZIP68 construct was used as the template for the mutagenesis with the following primer pairs, respectively: C320S-F and C320S-R, C182S-F and C182S-R. The clones that were confirmed by sequencing to contain the point mutations and were sub-cloned into the binary vector pYJHA (Chen et al., 2016) to generate *35S:bZIP68-HA*, *bZIP68C320S-HA*, and *35S:bZIP68C182S-HA*. To generate 35S:bZIP68C182S/320S-HA, the pMD-T19/bZIP68C320S was used as template for the mutagenesis with primer pairs C182S-F and C182S-R.

To generate *35S:bZIP68-FLAG*, the genomic region from the start codon to the last coding codon of *bZIP68* was amplified using the primer pairs SpeI-35SbZIP68-F and 35SbZIP68-SalI-R. After digestion with SpeI and SalI, the PCR products were inserted to the binary vector p35SFC which was modified from the vector pYJHA by replacing the 2xHA tag with the 3xFLAG tag.

For genetic complementation of the *bzip68* mutant, a 3.7-kb (-1170 to +2517) genomic fragment of *bZIP68* was PCR-amplified with the primers BamHI-combZIP68-F and combZIP68-PstI-R from Col-0 genomic DNA and cloned into a BamHI/PstI-digested pCAMBIA1300 vector (SnapGene, Chicago). The construct was transformed into the *bzip68*

mutant to yield the *bzip68*/Comp transgenic line. Multiple independent transgenic lines were identified and used for subsequent phenotypic analysis.

Confocal microscopic observation for subcellular localization of eYFP

For determining subcellular localization of the eYFP reporter, seedlings expressing various eYFP reporter constructs were observed under a confocal microscope (Leica TCS SP5 II) with 488-nm excitation and 500- to 530-nm emission. Seedlings were immersed in water (control) or 5 mM H_2O_2 solution and observed with the confocal microscope at different time points after the oxidant treatment.

Generation of transgenic Arabidopsis lines and transient expression in mesophyll protoplasts

Arabidopsis transformation was conducted via *Agrobacterium tumefaciens*-mediated transformation by using eh floral dipping method (Clough and Bent, 1998). The T2 and/ or later generations of the stable transgenic lines were selected and used for the YFP subcellular localization or phenotypic analysis.

Protoplast preparation and transient gene expression assay were performed according to the protocol from J Sheen lab (Yoo et al., 2007) with minor modifications. Four-week-old well-expanded rosette leaves of *bzip68-1* were used for preparing mesophyll protoplasts. After PEG-mediated transformation of protoplasts, the protoplasts were centrifugated at 200 g for 2 minutes, suspended in 1ml the suspension buffer (0.4 M mannitol 15 mM MgCl2, 4

mM MES (pH 5.7), and incubated in a plant growth chamber for 20 hrs. Ten ul of 500 mM H_2O_2 or 1M DTT stock solution was added to the protoplast suspension to the final concentration of 5 mM or 10 mM, respectively. An equal volume of suspension buffer was added to another tube of the protoplast suspension as a mock treatment. One hour later, the protoplasts were centrifugated and lysed in the protein extraction buffer without a reducing agent (50 mM Tris-HCl pH 7.4, 150 mM NaCl, 0.5 Triton X-100, 1 x protease inhibitor cocktail, 10% w/v sucrose). After centrifugation, the supernatant was used for Western blot analysis.

Phenotypic analysis under different treatments

Seeds were sown on plates which were put at 4 ºC for 3 days for cold stratification to synchronize germination and then placed in a growth chamber for germination and seedling growth under different conditions specified in the result section. All media were autoclaved for 15 minutes at 121 °C.

For MV treatment, 1 mM paraquat (Sigma-Aldrich, 36541) stock was added to the autoclaved ½ MS medium with 3% sucrose to different final concentrations. Seedlings were grown on plates vertically after 3-day stratification at 4 ºC.

All the phenotype analysis experiments were carried out using multiple plates or pots and the data presented in the report are exemplars of the experiments that have been repeated. Root length and leaf areas were measured using the image processing program ImageJ (https://imagej.nih.gov/ij/).

RNA isolation, reverse transcription PCR, and transcriptome analyses

Total RNA was extracted using the Plant RNA Isolation Mini kit (Agilent). For RT-PCR analysis, RNA (1 μg) was digested by DNase I (NEB, M0203L) and then reverse transcribed using the M-MLV Reverse Transcriptase (Affymetrix, 78306) with oligo (dT) primers (Affymetrix, 77405). For semi-quantitative PCR analysis, cDNAs were amplified for 26 cycles using the primers Semi-F and Semi-R for *bZIP68* and Act-F and Act-R for *Act2*.

Primers bZIP68-qF-1 and bZIP68-qR-1 were used to determine the *bZIP68* gene expression levels in *bzip68-1* and *bzip68-2* mutants for real-time PCR analysis using SYBR Premix Ex Taq (TaKaRa, DRR420A) on a Mx3000P Real-Time PCR detection system (Agilent Technologies). Signals were normalized to the reference gene *Ubiqutin10* using the Δ^{CT} method, and the relative expression level of a gene was calculated from the ratio of its levels in *bzip68* mutants to wildtype. The H_2O_2 and mock treatments of seedlings for RNA extraction were the same as for the RNA-seq analysis. Three biological replicates were included in the quantitative real-time RT-PCR analysis.

To prepare tissue samples for RNA-sequencing, 2-week-old seedlings grown on MS3 medium were gently spraying with 15 mL 5 mM H2O2 or H2O (mock) respectively and kept the plates standing vertically for 90 minutes before sample collecting. Three biological replicates were included for each treatment. Bar-coded mRNA libraries were constructed by BGI (Shenzhen, China) using the Illumina's reagents and protocols according to the manufacturer's instruction. Samples were sequenced on Illumina HiSeq 2500 system. Total reads were mapped to the Arabidopsis genome (TAIR10; www.arabidopsis.org) using the

TopHat 2.1.0 software (Trapnell et al., 2009). Read counts for every gene were generated using RSEM2.1.30 (Anders et al., 2015). Differentially expressed genes (DEGs) between samples were defined by DESeq2 (Love et al., 2014), based on adjusted *P*-value equal or smaller than 0.05. GO term enrichment analysis was conducted using the DAVID database (Dennis et al., 2003) based on modified Fisher Exact Test. Heatmaps was plotted using R (Version 3.2.3). Gene Ontology analysis and the functional categories were identified by using the annotation of the Arabidopsis genome (TAIR10; www.arabidopsis.org).

ChIP-seq assay and ChIP-qPCR

The ChIP assay was carried out according to the protocol from Joseph Ecker lab (Song et al., 2016) with slight modifications. Briefly, 3g seedlings of 8-day-old *35S: bZIP68-FLAG* and *35S: GFP-FLAG* (negative control) transgenic plants were cross-linked with 1% of formaldehyde. After the nucleus isolation, chromatin was sheared to around 0.2-1.0 kb using Diagenode Bioruptor and immunoprecipitated with 30 ul Pierce™ ChIP-grade Protein A/G Magnetic Beads (ThermoFisher, 26162) which were pre-bound with 15 ul monoclonal FLAG antibody (Sigma Aldrich, F1804). After reversing the cross-linked DNA-Protein complex, 50 ul DNA was purified using a ChIP DNA Clean & Concentrator™ kit (ZYMO research, D5205). At the same time, 30 ul sheared chromatin solution from the sonication product was collected as an input sample and subjected to reverse-crosslinking directly to bypass the immunoprecipitating process. The input sample was purified and eluted in 50 ul H_2O through the column (ZYMO research, D5205). Library preparation for next generation sequencing

was carried out according to the manufacturer's manual (CWBIO, CW2585S, NGS Fast DNA Library Prep Set for Illumina). The libraries were sent to Novogene company (Tianjin, China) and sequenced using the Illumina HiSEQ1500 platform. At least 6 GB raw sequencing data for each bar-coded sample was obtained.

For ChIP-qPCR, the DNA preparation was carried out as in ChIP-seq analysis, three biological replicates were included in the assay. For the PCR reaction, the promoter of *ACTIN7* was used as a reference and DNA amplification data for the ChIP samples were normalized to the INPUT samples. The enrichment values were calculated based on the following formula: Relative fold enrichment=$2^{\wedge\Delta \text{ Ct Target promoter (INPUT-IP)}}/2^{\wedge \Delta \text{ Ct ACT7 (INPUT-IP)}}$.

CHIP-Seq data analysis and motif finding

The reference genome sequence used for analyzing the ChIP-Seq data and motif finding was the *Arabidopsis thaliana* TAIR10 database. Enriched peak regions were identified using MACS-1.4.3 (Feng et al., 2012) with default parameters (-g 1.2e8 -p 1e-5 -w --space 50 -m 10,30 -s 49). Chipseeker (Yu et al., 2015) was applied to calculate average profiles of ChIP peaks binding to TSS regions, perform enrichment analysis, and peak annotation. The binding regions were searched for known motifs using Homer (Heinz et al., 2010) with an adjusted *p* value threshold of 0.01.

bZIP68 recombinant protein purification and EMSA

For bZIP 68 protein expression in *E. coli*, the coding region of bZIP68 including the stop codon was PCR amplified by the primers EcoRI_bZIP68_F and bZIP68_SalI_R and ligated to the plasmid pET32a to place the bZIP68 coding sequence to downstream of the Trx-His tags to make an in-frame fusion construct. The expression construct was transformed into the *E. coli* Rosetta (DE3) strain for expression. Bacteria were grown in the LB medium to OD_{600} of 0.8 at 37 ℃. After adding IPTG (to a concentration of 0.2 mM), the bacteria were grown at 18 ℃ for overnight. His-tagged bZAIP68 was purified using HisPur Ni-NTA Resin (ThermoFisher, 88222) packaged in 10 ml centrifuge column according to the manufacturer's instruction.

To prepare biotinylated probes for EMSA, the same amount of 54-bp biotinylated oligo was annealed with its reverse complemented oligo to form a double-strand probe. Competitor DNA was produced in the same way except that the both oligos were unbiotinylated. For the Protein-DNA binding assay, one microliter of 1uM biotinylated DNA probe was incubated with 10 ug His-bZIP68 protein in a 20 ul mixture containing 10 mM Hepes (pH7.9), 5mM Tris-HCl (pH8.0), 50 mM KCl, 5mM MgCl2, 2.5mM DTT, 5% glycerol, 0.5% bovine serum albumin, 0.05% NP40, and 50 ng/ul Poly(dI-dC)) for one hour at 37 ℃. The DNA probe/protein was separated on a 6% native PAGE gel containing 5% glycerol, then transferred to a nylon membrane, and detected by HRP-streptavidin (Thermo fisher, N100) according to the manufacturer's instruction. For competition, 5x or 50x unlabeled probes were co-incubated with the biotinylated probes in the binding mixture.

ACCESSION NUMBER

The ChIP-seq data and RNA-seq data have been submitted to the GEO database under the accession # GSE133900.

ACKNOWLEDGMENTS

The work was supported by Research Grants Council of Hong Kong (GRF grant no. 32-14-123 and AoE grant no. AoE/M-403/16 to Y.X.), by Hong Kong Baptist University's Strategic Development Fund (grant no. SDF15-1012-P04 to Y.X.) and Inter-institutional Collaborative Research Scheme (grant no. ICRS/16-17/04 to Y.X.), and by Shaanxi University of Chinese Medicine (grant no. 104080001 and 2019-QN01 to Y.L.).

The authors declare that there is no conflict of interest.

Author contributions

Y.X. conceived the original research plan and supervised the experiments. Y.L., W. L., and HL.Z. designed and performed the experiments, and H. Z. performed analysis of the RNA-seq and ChIP-seq data. All authors participated in writing the manuscript.

SHORT LEGENDS FOR SUPPORTING INFORMATION

Supplementary Figure S1. Oxidation of bZIP68 caused by the abiotic stresses

Supplementary Figure S2. Subcellular localization of the eYFP signal in seedlings expressing 35S:bZIP68-eYFP

Supplementary Figure S3. The genomic region containing *bZIP68* and transcript analysis of its two T-DNA insertion mutants

Supplementary Figure S4. Complementation of the slower growth phenotype of *bzip68* under various conditions by the *bZIP68* transgene.

Supplementary Figure S5. The bZIP68-binding regions chosen for EMSA

Supplementary Figure S6. Purification of His-bZIP68 fusion protein from *E. coli*

Supplementary Figure S7. A Venn diagram representation that compares the putative bZIP68 target genes from the ChIP-seq analysis and DGEs between *bzip68* and wildtype

Supplementary Table S1 and **Table S2.** bZIP68-bound peaks and associated genes from ChIP-seq analysis. Submitted as a separate file.

Supplementary Table S3. Enriched GO terms of the genes whose promoters were bound by bZIP68. Submitted as a separate file.

Supplementary Table S4. The list of DEGs. Submitted as a separate file.

Supplementary Table S5. Results of GO analysis on DEGs. Submitted as a separate file.

Supplementary Table S6. The list of 80 most up-regulated and down-regulated genes in the bzip68 mutant under low light. Submitted as a separate file.

Supplementary Table S7. The list of H_2O_2-responsive genes in wildtype. Submitted as a separate file.

Supplementary Table S8. Enriched GO terms among the DEGs from the comparison between H_2O_2- and mock-treated WT seedlings.

Supplementary Table S9. List of the primers used in this study.

LITERATURE CITED

Anders, S., Pyl, P.T., and Huber, W. (2015). HTSeq--a Python framework to work with high-throughput sequencing data. Bioinformatics **31,** 166-169.

Apel, K., and Hirt, H. (2004). Reactive oxygen species: metabolism, oxidative stress, and signal transduction. Annu Rev Plant Biol **55,** 373-399.

Babbs, C.F., Pham, J.A., and Coolbaugh, R.C. (1989). Lethal Hydroxyl Radical Production in Paraquat-Treated Plants. Plant Physiol. **90,** 1267-1270.

Benjamins, R., Ampudia, C.S., Hooykaas, P.J., and Offringa, R. (2003). PINOID-mediated signaling involves calcium-binding proteins. Plant Physiol **132,** 1623-1630.

Brunkard, J.O., Runkel, A.M., and Zambryski, P.C. (2015). Chloroplasts extend stromules independently and in response to internal redox signals. Proc. Natl. Acad. Sci. U. S. A. **112,** 10044-10049.

Cai, X.T., Xu, P., Zhao, P.X., Liu, R., Yu, L.H., and Xiang, C.B. (2014). Arabidopsis ERF109 mediates cross-talk between jasmonic acid and auxin biosynthesis during lateral root formation. Nat Commun **5,** 5833.

Caplan, J.L., Kumar, A.S., Park, E., Padmanabhan, M.S., Hoban, K., Modla, S., Czymmek, K., and Dinesh-Kumar, S.P. (2015). Chloroplast Stromules Function during Innate Immunity. Dev Cell **34,** 45-57.

Chen, B., Niu, F., Liu, W.Z., Yang, B., Zhang, J., Ma, J., Cheng, H., Han, F., and Jiang, Y.Q. (2016). Identification, cloning and characterization of R2R3-MYB gene family in canola (Brassica napus L.) identify a novel member modulating ROS accumulation and hypersensitive-like cell death. DNA Res **23,** 101-114.

Chen, D., Xu, G., Tang, W., Jing, Y., Ji, Q., Fei, Z., and Lin, R. (2013). Antagonistic basic helix-loop-helix/bZIP transcription factors form transcriptional modules that integrate light and reactive oxygen species signaling in Arabidopsis. Plant Cell **25,** 1657-1673.

Chia, L.S., McRae, D.G., and Thompson, J.E. (1982). Light-dependence of paraquat-initiated membrane deterioration in bean plants. Evidence for the involvement of superoxide. Physiol. Plant. **56,** 492-499.

Clough, S.J., and Bent, A.F. (1998). Floral dip: a simplified method for Agrobacterium-mediated transformation of Arabidopsis thaliana. Plant J **16,** 735-743.

Collins, Y., Chouchani, E.T., James, A.M., Menger, K.E., Cocheme, H.M., and Murphy, M.P. (2012). Mitochondrial redox signalling at a glance. J Cell Sci **125,** 801-806.

D'Autreaux, B., and Toledano, M.B. (2007). ROS as signalling molecules: mechanisms that generate specificity in ROS homeostasis. Nat Rev Mol Cell Biol **8,** 813-824.

Deng, Y., Humbert, S., Liu, J.X., Srivastava, R., Rothstein, S.J., and Howell, S.H. (2011). Heat induces the splicing by IRE1 of a mRNA encoding a transcription factor involved in the unfolded protein response in Arabidopsis. Proc Natl Acad Sci U S A **108,** 7247-7252.

Dennis, G., Jr., Sherman, B.T., Hosack, D.A., Yang, J., Gao, W., Lane, H.C., and Lempicki, R.A. (2003). DAVID: Database for Annotation, Visualization, and Integrated Discovery. Genome Biol **4,** P3.

Dietz, K.J. (2014). Redox regulation of transcription factors in plant stress acclimation and development. Antioxid Redox Signal **21,** 1356-1372.

Ezer, D., Shepherd, S.J.K., Brestovitsky, A., Dickinson, P., Cortijo, S., Charoensawan, V., Box, M.S., Biswas, S., Jaeger, K.E., and Wigge, P.A. (2017). The G-Box Transcriptional Regulatory Code in Arabidopsis. Plant Physiol **175,** 628-640.

Feng, J., Liu, T., Qin, B., Zhang, Y., and Liu, X.S. (2012). Identifying ChIP-seq enrichment using MACS. Nat Protoc **7,** 1728-1740.

Finkel, T. (2011). Signal transduction by reactive oxygen species. J Cell Biol **194,** 7-15.

Flematti, G.R., Dixon, K.W., and Smith, S.M. (2015). What are karrikins and how were they 'discovered' by plants? BMC Biol **13,** 108.

Foyer, C.H., and Noctor, G. (2005). Redox homeostasis and antioxidant signaling: a metabolic interface between stress perception and physiological responses. Plant Cell **17,** 1866-1875.

Garreton, V., Carpinelli, J., Jordana, X., and Holuigue, L. (2002). The as-1 promoter element is an oxidative stress-responsive element and salicylic acid activates it via oxidative species. Plant Physiol **130,** 1516-1526.

Georgiou, G. (2002). How to flip the (redox) switch. Cell **111,** 607-610.

Heinz, S., Benner, C., Spann, N., Bertolino, E., Lin, Y.C., Laslo, P., Cheng, J.X., Murre, C., Singh, H., and Glass, C.K. (2010). Simple combinations of lineage-determining transcription factors prime cis-regulatory elements required for macrophage and B cell identities. Mol. Cell **38,** 576-589.

Herrera-Vasquez, A., Salinas, P., and Holuigue, L. (2015). Salicylic acid and reactive oxygen species interplay in the transcriptional control of defense genes expression. Front Plant Sci **6,** 171.

Ho, S.N., Hunt, H.D., Horton, R.M., Pullen, J.K., and Pease, L.R. (1989). Site-directed mutagenesis by overlap extension using the polymerase chain reaction. Gene **77,** 51-59.

Hsieh, W.P., Hsieh, H.L., and Wu, S.H. (2012). Arabidopsis bZIP16 transcription factor integrates light and hormone signaling pathways to regulate early seedling development. Plant Cell **24,** 3997-4011.

Jakoby, M., Weisshaar, B., Droge-Laser, W., Vicente-Carbajosa, J., Tiedemann, J., Kroj, T., and Parcy, F. (2002). bZIP transcription factors in Arabidopsis. Trends Plant Sci **7,** 106-111.

Kuge, S., Jones, N., and Nomoto, A. (1997). Regulation of yAP-1 nuclear localization in response to oxidative stress. EMBO J **16,** 1710-1720.

Lai, Y.S., Stefano, G., Zemelis-Durfee, S., Ruberti, C., Gibbons, L., and Brandizzi, F. (2018). Systemic signaling contributes to the unfolded protein response of the plant endoplasmic reticulum. Nat Commun **9,** 3918.

Lamb, C., and Dixon, R.A. (1997). The Oxidative Burst in Plant Disease Resistance. Annu Rev Plant Physiol Plant Mol Biol **48,** 251-275.

Lau, O.S., Davies, K.A., Chang, J., Adrian, J., Rowe, M.H., Ballenger, C.E., and Bergmann, D.C. (2014). Direct roles of SPEECHLESS in the specification of stomatal self-renewing cells. Science **345,** 1605-1609.

Lindermayr, C., Sell, S., Muller, B., Leister, D., and Durner, J. (2010). Redox regulation of the NPR1-TGA1 system of Arabidopsis thaliana by nitric oxide. Plant Cell **22,** 2894-2907.

Liu, P., Zhang, H., Wang, H., and Xia, Y. (2014). Identification of redox-sensitive cysteines in the Arabidopsis proteome using OxiTRAQ, a quantitative redox proteomics method. Proteomics **14,** 750-762.

Love, M.I., Huber, W., and Anders, S. (2014). Moderated estimation of fold change and dispersion for RNA-seq data with DESeq2. Genome Biol **15,** 550.

Lu, Y., Li, C., Wang, H., Chen, H., Berg, H., and Xia, Y. (2011). AtPPR2, an Arabidopsis pentatricopeptide repeat protein, binds to plastid 23S rRNA and plays an important role in the first mitotic division during gametogenesis and in cell proliferation during embryogenesis.

Plant J. **67,** 13-25.

Marino, D., Dunand, C., Puppo, A., and Pauly, N. (2012). A burst of plant NADPH oxidases. Trends Plant Sci **17,** 9-15.

Matsuo, M., and Oelmüller, R. (2015). REDOX RESPONSIVE TRANSCRIPTION FACTOR1 is involved in age-dependent and systemic stress signaling. Plant signaling & behavior **10,** e1051279-e1051279.

Meng, Y., Shuai, H., Luo, X., Chen, F., Zhou, W., Yang, W., and Shu, K. (2016). Karrikins: Regulators Involved in Phytohormone Signaling Networks during Seed Germination and Seedling Development. Front Plant Sci **7,** 2021.

Menkens, A.E., Schindler, U., and Cashmore, A.R. (1995). The G-box: a ubiquitous regulatory DNA element in plants bound by the GBF family of bZIP proteins. Trends Biochem Sci **20,** 506-510.

Moller, I.M., Jensen, P.E., and Hansson, A. (2007). Oxidative modifications to cellular components in plants. Annu Rev Plant Biol **58,** 459-481.

Morffy, N., Faure, L., and Nelson, D.C. (2016). Smoke and Hormone Mirrors: Action and Evolution of Karrikin and Strigolactone Signaling. Trends Genet **32,** 176-188.

Mou, Z., Fan, W., and Dong, X. (2003). Inducers of plant systemic acquired resistance regulate NPR1 function through redox changes.[see comment]. Cell **113,** 935-944.

Mudgil, Y., Uhrig, J.F., Zhou, J., Temple, B., Jiang, K., and Jones, A.M. (2009). Arabidopsis N-MYC DOWNREGULATED-LIKE1, a positive regulator of auxin transport in a G protein-mediated pathway. Plant Cell **21,** 3591-3609.

Nishizawa, A., Yabuta, Y., and Shigeoka, S. (2008). Galactinol and raffinose constitute a novel function to protect plants from oxidative damage. Plant Physiol **147,** 1251-1263.

Oh, E., Zhu, J.Y., and Wang, Z.Y. (2012). Interaction between BZR1 and PIF4 integrates brassinosteroid and environmental responses. Nat Cell Biol **14,** 802-809.

Pfeiffer, A., Shi, H., Tepperman, J.M., Zhang, Y., and Quail, P.H. (2014). Combinatorial complexity in a transcriptionally centered signaling hub in Arabidopsis. Mol Plant **7,** 1598-1618.

Provost, C., Choufani, F., Avedanian, L., Bkaily, G., Gobeil, F., and Jacques, D. (2010). Nitric oxide and reactive oxygen species in the nucleus revisited. Can J Physiol Pharmacol **88,** 296-304.

Schieber, M., and Chandel, N.S. (2014). ROS function in redox signaling and oxidative stress. Curr Biol **24,** R453-462.

Schindler, U., Terzaghi, W., Beckmann, H., Kadesch, T., and Cashmore, A.R. (1992). DNA binding site preferences and transcriptional activation properties of the Arabidopsis transcription factor GBF1. EMBO J **11,** 1275-1289.

Shaikhali, J., Noren, L., de Dios Barajas-Lopez, J., Srivastava, V., Konig, J., Sauer, U.H., Wingsle, G., Dietz, K.J., and Strand, A. (2012). Redox-mediated mechanisms regulate DNA binding activity of the G-group of basic region leucine zipper (bZIP) transcription factors in Arabidopsis. J Biol Chem **287,** 27510-27525.

Shen, H., Cao, K., and Wang, X. (2008). AtbZIP16 and AtbZIP68, two new members of GBFs, can interact with other G group bZIPs in Arabidopsis thaliana. BMB Rep **41,** 132-138.

Siberil, Y., Doireau, P., and Gantet, P. (2001). Plant bZIP G-box binding factors. Modular structure and activation mechanisms. Eur J Biochem **268,** 5655-5666.

Smykowski, A., Zimmermann, P., and Zentgraf, U. (2010). G-Box binding factor1 reduces CATALASE2 expression and regulates the onset of leaf senescence in Arabidopsis. Plant Physiol **153,** 1321-1331.

Song, L., Koga, Y., and Ecker, J.R. (2016). Profiling of transcription factor binding events by chromatin immunoprecipitation sequencing (ChIP-seq). Curr Protoc Plant Biol **1,** 293-306.

Toledo-Ortiz, G., Johansson, H., Lee, K.P., Bou-Torrent, J., Stewart, K., Steel, G., Rodriguez-Concepcion, M., and Halliday, K.J. (2014). The HY5-PIF regulatory module coordinates light and temperature control of photosynthetic gene transcription. PLoS Genet **10,** e1004416.

Trapnell, C., Pachter, L., and Salzberg, S.L. (2009). TopHat: discovering splice junctions with RNA-Seq. Bioinformatics **25,** 1105-1111.

Waters, M.T., Scaffidi, A., Sun, Y.K., Flematti, G.R., and Smith, S.M. (2014). The karrikin response system of Arabidopsis. Plant J **79,** 623-631.

Xia, X.J., Zhou, Y.H., Shi, K., Zhou, J., Foyer, C.H., and Yu, J.Q. (2015). Interplay between reactive oxygen species and hormones in the control of plant development and stress tolerance. J Exp Bot **66,** 2839-2856.

Yoo, S.D., Cho, Y.H., and Sheen, J. (2007). Arabidopsis mesophyll protoplasts: a versatile cell system for transient gene expression analysis. Nat Protoc **2,** 1565-1572.

Yu, G., Wang, L.G., and He, Q.Y. (2015). ChIPseeker: an R/Bioconductor package for ChIP peak annotation, comparison and visualization. Bioinformatics **31,** 2382-2383.

Yu, X., Li, L., Zola, J., Aluru, M., Ye, H., Foudree, A., Guo, H., Anderson, S., Aluru, S., Liu, P., Rodermel, S., and Yin, Y. (2011). A brassinosteroid transcriptional network revealed by genome-wide identification of BESI target genes in Arabidopsis thaliana. Plant J **65,** 634-646.

Zhiponova, M.K., Morohashi, K., Vanhoutte, I., Machemer-Noonan, K., Revalska, M., Van Montagu, M., Grotewold, E., and Russinova, E. (2014). Helix-loop-helix/basic helix-loop-helix transcription factor network represses cell elongation in Arabidopsis through an apparent incoherent feed-forward loop. Proc Natl Acad Sci U S A **111,** 2824-2829.

Table 1. Most significantly enriched GO terms among DEGs affected by *bzip68* mutation

bzip68/wildtype under low light		
Up-Regulated		
Gene Ontology Term	Count	*P*-Value
GO:0009611~response to wounding	59	5.95E-24
GO:0010200~response to chitin	44	5.10E-20
GO:0006468~protein phosphorylation	126	5.13E-19
GO:0009753~response to jasmonic acid	38	1.19E-12
GO:0006952~defense response	88	2.26E-11
GO:0042546~cell wall biogenesis	22	3.41E-11
GO:0042742~defense response to bacterium	48	3.16E-10
GO:0009617~response to bacterium	27	4.93E-10
GO:0009414~response to water deprivation	47	1.44E-09
GO:0010411~xyloglucan metabolic process	17	1.77E-09
Down-Regulated		
Gene Ontology Term	Count	*P*-Value
GO:0006351~transcription, DNA-templated	98	1.02E-11
GO:0006355~regulation of transcription, DNA-templated	106	1.09E-11
GO:0009733~response to auxin	29	1.75E-09
GO:0009926~auxin polar transport	12	1.40E-07
GO:0009734~auxin-activated signaling pathway	20	4.30E-07
GO:0009751~response to salicylic acid	18	4.73E-07
GO:0009813~flavonoid biosynthetic process	17	9.45E-07
GO:0010224~response to UV-B	11	2.99E-06
GO:0080167~response to karrikin	15	5.00E-06
GO:0009718~anthocyanin-containing compound biosynthetic process	7	5.47E-06

Table 2. Most significantly enriched GO terms among ROS-responsive genes in wildtype seedlings

ROS-induced genes

Gene Ontology Term	Count	*P*-Value
GO:0009408~response to heat	43	8.06E-18
GO:0009737~response to abscisic acid	66	1.73E-15
GO:0042742~defense response to bacterium	53	5.15E-15
GO:0010200~response to chitin	34	1.78E-13
GO:0006468~protein phosphorylation	97	5.66E-11
GO:0009409~response to cold	48	8.49E-11
GO:0009414~response to water deprivation	44	1.01E-09
GO:0009611~response to wounding	35	3.97E-09
GO:0042542~response to hydrogen peroxide	17	1.99E-08
GO:0006952~defense response	73	2.31E-08

ROS-suppressed genes

Gene Ontology Term	Count	*P*-Value
GO:0009753~response to jasmonic acid	26	7.03E-10
GO:0006949~syncytium formation*	9	1.82E-08
GO:0010114~response to red light	15	1.93E-08
GO:0009992~cellular water homeostasis	12	6.24E-08
GO:0006355~regulation of transcription, DNA-templated	126	9.54E-08
GO:0080167~response to karrikin	20	2.71E-07
GO:0034220~ion transmembrane transport	10	4.79E-07
GO:0007623~circadian rhythm	17	5.50E-07
GO:0009739~response to gibberellin	17	7.32E-07
GO:0006833~water transport	7	1.03E-06

*The term syncytium, mainly used in animals, refers to mitotic cell division without cytokinesis.

FIGURE LEGENDS

Figure 1. bZIP68 undergoes in-vivo oxidation under H_2O_2 treatment which is dependent on its Cys320 residue

Shown are the results from Western blot analysis for detection of bZIP68-HA, bZIP68C320S, and bZIP68C182S expressed in protoplasts with or without H_2O_2 treatment. Proteins were extracted and dissolved in the extraction buffer without a reducing agent. The proteins were detected by the anti-HA antibodies.

(a) Proteins extracted from the protoplasts expressing bZIP68-HA under the indicated treatments were added to the loading buffer with or without DTT for SDS-PAGE analysis. The lower panel was a part of the SDS-PAGE gel stained with the Coomassie Blue dye.

(b) Proteins were from the protoplasts that were transformed with the wildtype bZIP68 or its mutated forms and were treated with H_2O_2 or with the buffer only. The lower panel was a part of the SDS-PAGE gel stained with the Coomassie Blue dye.

Figure 2. Subcellular localization of bZIP68-eYFP in root cells of the seedlings under the control (normal) condition and under H_2O_2 treatment.

(a-b) The YFP fluorescence images of root cells of the *bZIP68pro:bZIP68-eYFP* seedlings under the control condition (a, b) and after ROS treatment (5 mM H_2O_2 for 30 minutes) (c, d). Bars = 5 μm.

(e-h) The YFP fluorescence images of root cells of the *bZIP68pro:bZIP68C320S-eYFP* seedlings under the control condition (e,f) and after ROS treatment (5 mM H2O2 for 30 minutes) (g, h). b,d,f,h are the fluorescence images and a,c,e,g are the florescence images merged with the bight field images. Bars = 5 μm.

Multiple transgenic lines were observed and representative photos are showed in the figure.

Figure 3. The *bzip68* mutation leads to slower seedling growth under various growth conditions.

(a-c) Four-week-old (a) and 6-week-old (c) *bzip68* mutants and wildtype (WT) plants grown in soil. (b) is statistical analysis of leaf areas of 4-week-old plants of the different genotypes from multiple pots. * and ** represent statistically significant ($p \leq 0.05$) and highly significant ($p \leq 0.01$) difference, respectively. The difference in leaf areas between *bzip68-1* and *bzip68-2* was also statistically significant.

(d-f) Six-day-old seedlings grown on MS1 (d) or MS3 (e) medium. (f) is statistical analysis of root length of seedlings from multiple plates under the condition of (d) and (e).

(g-i) Seedlings grown on MS3 medium under low light (30 mol m^{-2} sec^{-1}). The seedlings were photographed 2 days (D2) and 5 days (D5) after germination. (i) is statistical analysis of seedlings from multiple plates under the conditions of g-h.

(j-l) Seedlings grown under low temperature (15 °C) on the MS3 with 3% sucrose. The seedlings were photographed 3 days (D3) and 7 days (D7) after germination. (l) is statistical analysis of seedlings from multiple plates under the conditions of j-k.

Error bars represent SE (n = 20). A Student's t-test was used for comparisons marked in the figure; *p<0.05 and **p<0.01. Similar results were obtained from multiple experiments and representative photos are showed in the figure.

Figure 4. The *bzip68* mutant was less sensitive than wildtype to MV-caused seedling growth inhibition.

(a) Seven-day-old seedlings grown on the MS3 medium with or without the different concentration of MV. *bZIP68-FLAG*: the Col-0 transgenic line expressing the *35S:bZIP68-FLAG* transgene.

(b) Statistical analysis of seedlings from multiple plates under the conditions of (a). Error bars represent SE (n = 20) from the Student's t-test. The different letters above the error bars represent statistically significant difference (p<0.05). Similar results were obtained from multiple experiments and representative photos are showed in the figure.

Figure 5. ChIP-seq for genome-wide analysis of bZIP68 binding sites

(a, b) Positions of the bZIP68 binding sites relative to TSS (A) and distribution of bZIP68 binding sties relative to gene structures (b). Promoter (<=1kb): -1.0 kb to +500b relative to TSS.

(c) Motif discovery using HOMER reveals that the G-box (CACGTG) and G-box-like motifs are enriched at the bZIP68 binding sites.

(d) Enriched GO terms of bZIP68 targets.

Figure 6. ChIP-qPCR and EMSA analyses of bZIP68-binding sites

(a) ChIP-qPCR verification of bZIP68-binding regions associated with the promoter regions of 14 genes. The promoter region of *ACTIN7* was used as a reference.

(b) EMSA assay to detect binding of His-bZIP68 to the promoter regions from 6 genes. 5x or 50x of competitor probe DNA (unlabeled) were added as control in the assay. The left and right panels were the results from two separate experiments.

Figure 7. Comparison of gene expression profiles affected by the *bzip68* mutation and by H2O2 treatment

(a) Heatmap of differentially expressed genes (DEGs) indicates that the *bzip68* mutation ehances expression of ROS-responsive genes. Shown is Heatmap from hierarchical clustering of 5,059 DEGs (with adjusted *P* values of ≤ 0.05, shown in FPKM). The DEGs were from at least one of the following comparisons: between WT and *bzip68* under low light, between mock-treated mutant and mock-treated WT under normal light, or between ROS-treated and mock-treated plants of the same genotype. Three biological replicates were included for each treatment. Gene clusters were subjected to the DAVID web server for Gene Ontology analysis.

(b) Comparison of the transcript levels of the indicated genes between *bzip68* and wildtype seedlings from the RNA-seq data and the RT-qPCR data. The seedlings were under normal growth conditions. *UBQ10* was used as reference.

(c) Comparison of the transcript levels of the four genes in *bzip68* and wildtype seedlings with and without H_2O_2 treatment. The error bars represent SD.B, Oxidation of bZIP68 under stress leads to its inactivation and/or translocation to the cytoplasm to enhance expression of stress tolerance genes but reduce expression of growth-promoting genes.

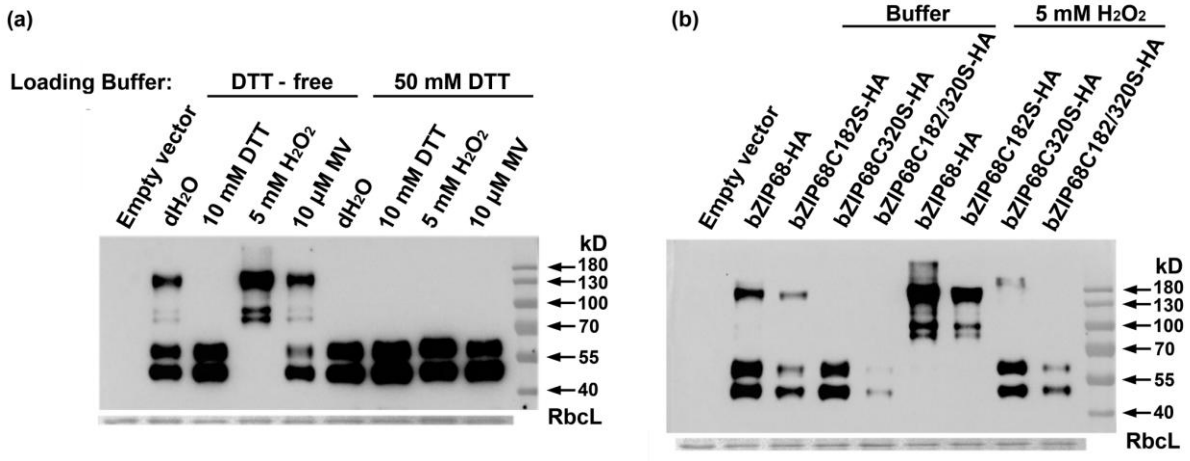

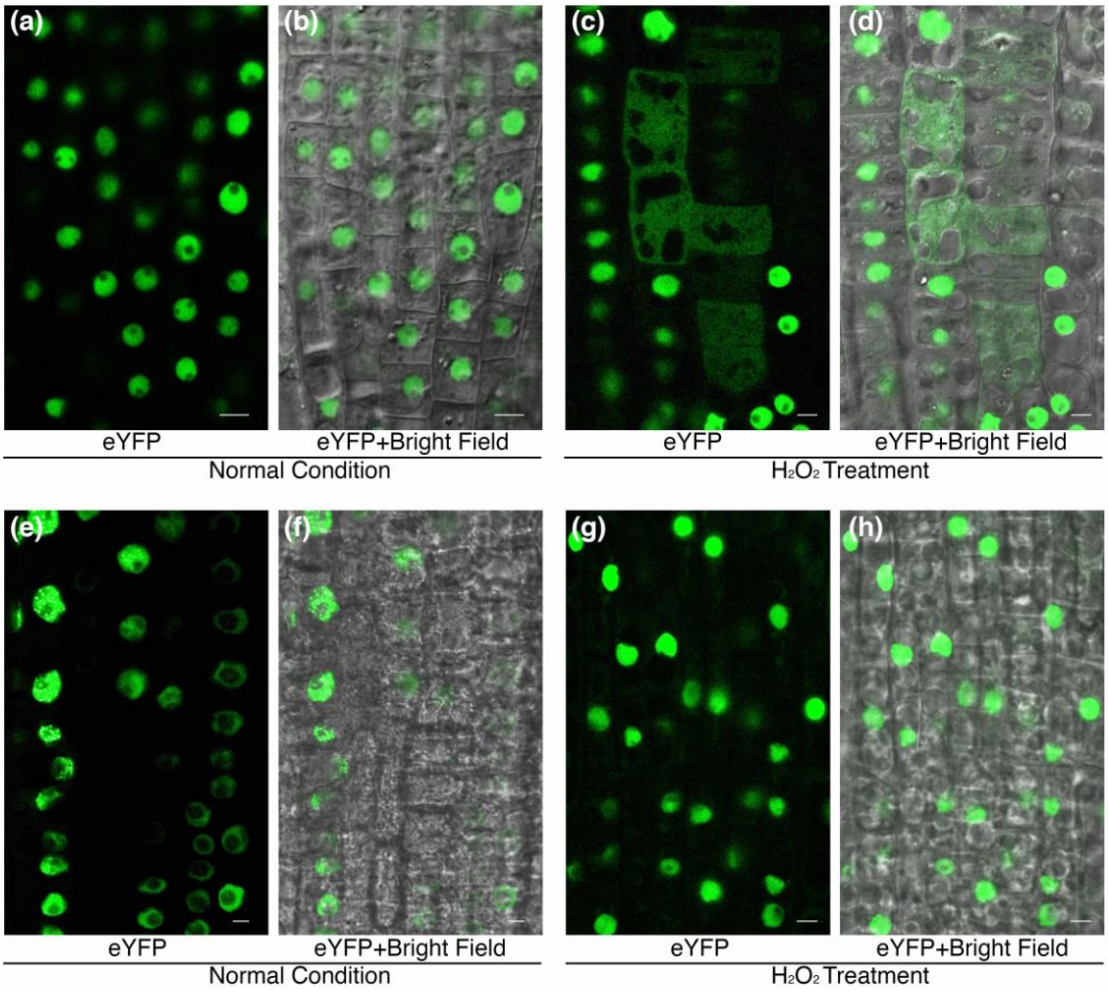

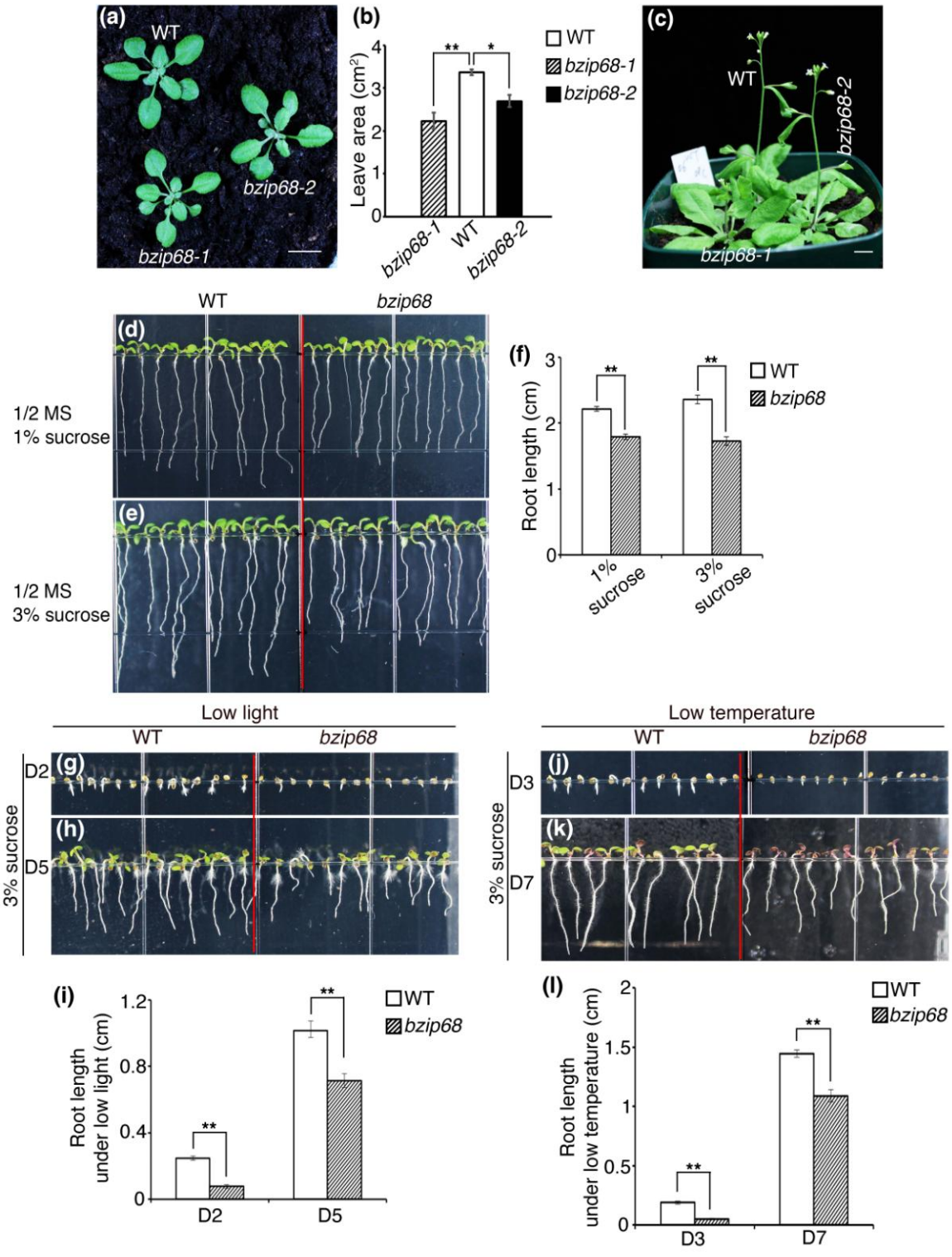

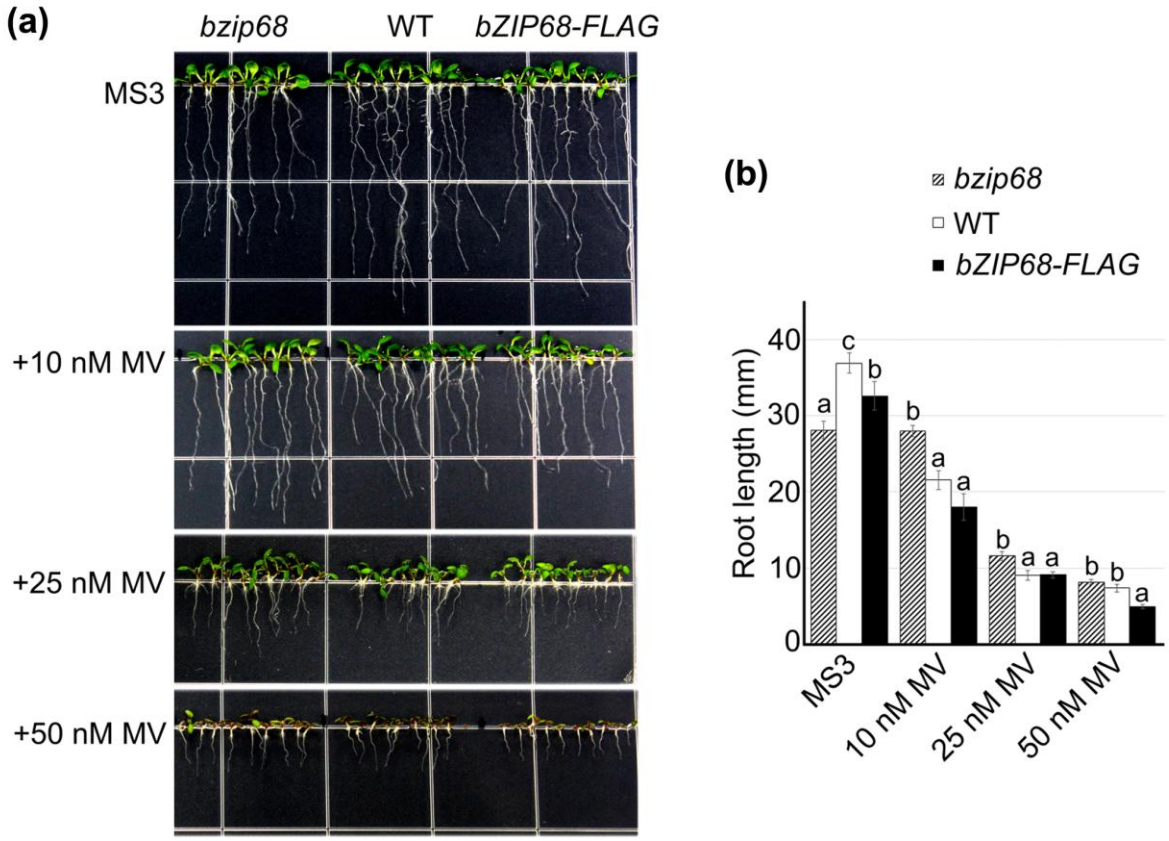

(a)

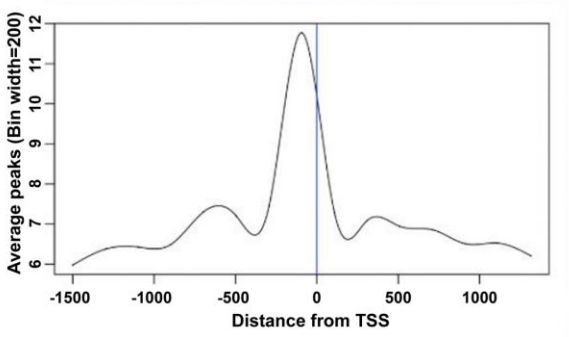

(b)

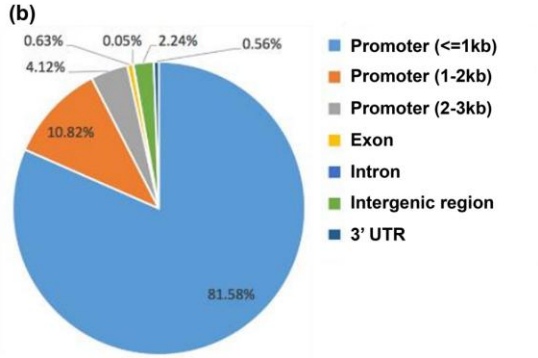

(c)

LOGO	Motif Name	P-value	% of Target Sequences with Motif
	G-box	1.00E-139	32.34%
	SPCH(bHLH)	1.00E-158	51.92%
	PIF4(bHLH)	1.00E-92	36.01%
	IBL1(bHLH)	1.00E-84	43.36%
	PIF5ox(bHLH)	1.00E-76	31.21%

(d)